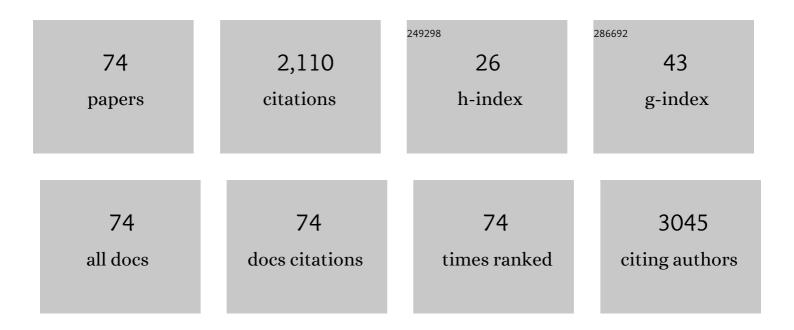
Cheng Peng

List of Publications by Year in descending order

Source: https://exaly.com/author-pdf/8440190/publications.pdf Version: 2024-02-01



CHENC PENC

#	Article	IF	CITATIONS
1	Human Exposure Assessment of Mixed Metal/Loids at and Near Mega-Scale Open Beaching Shipwrecking Activities in Bangladesh. Exposure and Health, 2023, 15, 69-84.	2.8	2
2	Combined effects of mixed per- and polyfluoroalkyl substances on the Nrf2-ARE pathway in ARE reporter-HepG2 cells. Journal of Hazardous Materials, 2022, 421, 126827.	6.5	16
3	Microcrystalline silica particles induce inflammatory response via pyroptosis in primary human respiratory epithelial cells. Environmental Toxicology, 2022, 37, 385-400.	2.1	9
4	Activation of pyroptosis and ferroptosis is involved in the hepatotoxicity induced by polystyrene microplastics in mice. Chemosphere, 2022, 291, 132944.	4.2	78
5	Integrative transcriptomic and proteomic analysis reveals mechanisms of silica-induced pulmonary fibrosis in rats. BMC Pulmonary Medicine, 2022, 22, 13.	0.8	7
6	Ligand-independent activation of AhR by hydroquinone mediates benzene-induced hematopoietic toxicity. Chemico-Biological Interactions, 2022, 355, 109845.	1.7	4
7	Pollution characteristics and health risk assessment of PM2.5-bound arsenic: a 7-year observation in the urban area of Jinan, China. Environmental Geochemistry and Health, 2022, 44, 4619-4630.	1.8	3
8	Understanding the mechanisms of silica nanoparticles for nanomedicine. Wiley Interdisciplinary Reviews: Nanomedicine and Nanobiotechnology, 2021, 13, e1658.	3.3	35
9	Toluene diisocyanate-induced inflammation and airway remodeling involves autophagy in human bronchial epithelial cells. Toxicology in Vitro, 2021, 70, 105040.	1.1	7
10	Lead-induced cardiomyocytes apoptosis by inhibiting gap junction intercellular communication via autophagy activation. Chemico-Biological Interactions, 2021, 337, 109331.	1.7	20
11	Assessing the human health risks of per- and polyfluoroalkyl substances: A need for greater focus on their interactions as mixtures. Journal of Hazardous Materials, 2021, 407, 124863.	6.5	87
12	OUP accepted manuscript. Annals of Work Exposures and Health, 2021, , .	0.6	0
13	Emodin attenuates silica-induced lung injury by inhibition of inflammation, apoptosis and epithelial-mesenchymal transition. International Immunopharmacology, 2021, 91, 107277.	1.7	36
14	Activation of Nrf2/ <scp>HO</scp> â€1 signaling pathway attenuates <scp>ROS</scp> â€mediated autophagy induced by silica nanoparticles in <i>H9c2</i> cells. Environmental Toxicology, 2021, 36, 1389-1401.	2.1	9
15	Dynamic assessing silica particle-induced pulmonary fibrosis and associated regulation of long non-coding RNA expression in Wistar rats. Genes and Environment, 2021, 43, 23.	0.9	6
16	Exosomes derived from bone marrow mesenchymal stem cells reverse epithelial-mesenchymal transition potentially via attenuating Wnt/ \hat{l}^2 -catenin signaling to alleviate silica-induced pulmonary fibrosis. Toxicology Mechanisms and Methods, 2021, 31, 655-666.	1.3	17
17	Metformin Attenuates Silica-Induced Pulmonary Fibrosis by Activating Autophagy via the AMPK-mTOR Signaling Pathway. Frontiers in Pharmacology, 2021, 12, 719589.	1.6	27
18	The role of HMGB1 on TDI-induced NLPR3 inflammasome activation via ROS/NF-κB pathway in HBE cells. International Immunopharmacology, 2021, 98, 107859.	1.7	7

CHENG PENG

#	Article	IF	CITATIONS
19	Evaluation of the individual and combined toxicity of perfluoroalkyl substances to human liver cells using biomarkers of oxidative stress. Chemosphere, 2021, 281, 130808.	4.2	45
20	Comprehensive analysis of differences of N6-methyladenosine of lncRNAs between atrazine-induced and normal Xenopus laevis testis. Genes and Environment, 2021, 43, 49.	0.9	3
21	Pollution characteristics and chronic health risk assessment of metals and metalloids in ambient PM2.5 in Licheng District, Jinan, China. Environmental Geochemistry and Health, 2020, 42, 1803-1815.	1.8	20
22	Distinct m6A methylome profiles in poly(A) RNA from Xenopus laevis testis and that treated with atrazine. Chemosphere, 2020, 245, 125631.	4.2	19
23	Combined effects and toxicological interactions of perfluoroalkyl and polyfluoroalkyl substances mixtures in human liver cells (HepG2). Environmental Pollution, 2020, 263, 114182.	3.7	78
24	Epimedium Polysaccharide Ameliorates Benzene-Induced Aplastic Anemia in Mice. Evidence-based Complementary and Alternative Medicine, 2020, 2020, 1-12.	0.5	3
25	Comparative proteomic analysis of silica-induced pulmonary fibrosis in rats based on tandem mass tag (TMT) quantitation technology. PLoS ONE, 2020, 15, e0241310.	1.1	16
26	Title is missing!. , 2020, 15, e0241310.		0
27	Title is missing!. , 2020, 15, e0241310.		Ο
28	Title is missing!. , 2020, 15, e0241310.		0
29	Title is missing!. , 2020, 15, e0241310.		0
30	Title is missing!. , 2020, 15, e0241310.		0
31	Title is missing!. , 2020, 15, e0241310.		Ο
32	Silica nanoparticles induce cardiomyocyte apoptosis via the mitochondrial pathway in rats following intratracheal instillation. International Journal of Molecular Medicine, 2019, 43, 1229-1240.	1.8	22
33	Mechanism of cell death induced by silica nanoparticles in hepatocyte cells is by apoptosis. International Journal of Molecular Medicine, 2019, 44, 903-912.	1.8	30
34	Thymic stromal lymphopoietin (TSLP) and Toluene-diisocyanate-induced airway inflammation: Alleviation by TSLP neutralizing antibody. Toxicology Letters, 2019, 317, 59-67.	0.4	6
35	Analysis of long nonâ€coding RNA involved in atrazineâ€induced testicular degeneration of <scp><i>Xenopus laevis</i></scp> . Environmental Toxicology, 2019, 34, 505-512.	2.1	14
36	Profiling long non-coding RNA changes in silica-induced pulmonary fibrosis in rat. Toxicology Letters, 2019, 310, 7-13.	0.4	27

CHENG PENG

#	Article	IF	CITATIONS
37	Long-term exposure to crotonaldehyde causes heart and kidney dysfunction through induction of inflammatory and oxidative damage in male Wistar rats. Toxicology Mechanisms and Methods, 2019, 29, 263-275.	1.3	12
38	Identification of circular RNAs and their alterations involved in developing male Xenopus laevis chronically exposed to atrazine. Chemosphere, 2018, 200, 295-301.	4.2	30
39	Genotoxicity evaluation of multi-component mixtures of polyaromatic hydrocarbons (PAHs), arsenic, cadmium, and lead using flow cytometry based micronucleus test in HepG2 cells. Mutation Research - Genetic Toxicology and Environmental Mutagenesis, 2018, 827, 9-18.	0.9	12
40	Transplantation of adipose-derived mesenchymal stem cells attenuates pulmonary fibrosis of silicosis via anti-inflammatory and anti-apoptosis effects in rats. Stem Cell Research and Therapy, 2018, 9, 110.	2.4	91
41	Relationship between occupational noise exposure and the risk factors of cardiovascular disease in China. Medicine (United States), 2018, 97, e11720.	0.4	34
42	Bone marrow mesenchymal stromal cells attenuate silica-induced pulmonary fibrosis potentially by attenuating Wnt/β-catenin signaling in rats. Stem Cell Research and Therapy, 2018, 9, 311.	2.4	34
43	Validation and bioinformatics analysis of differentially expressed circRNAs involved in developing male Xenopus laevis chronically exposed to atrazine. Data in Brief, 2018, 18, 1282-1291.	0.5	1
44	Interaction effects of As, Cd and Pb on their respective bioaccessibility with time in co-contaminated soils assessed by the Unified BARGE Method. Environmental Science and Pollution Research, 2017, 24, 5585-5594.	2.7	9
45	Endosulfan induces cell dysfunction through cycle arrest resulting from DNA damage and DNA damage and DNA damage damage response signaling pathways. Science of the Total Environment, 2017, 589, 97-106.	3.9	12
46	Endosulfan inhibits proliferation through the Notch signaling pathway in human umbilical vein endothelial cells. Environmental Pollution, 2017, 221, 26-36.	3.7	15
47	Inhibition of gap junction intercellular communication is involved in silica nanoparticles-induced H9c2 cardiomyocytes apoptosis via the mitochondrial pathway. International Journal of Nanomedicine, 2017, Volume 12, 2179-2188.	3.3	42
48	The Role of Epigenetic Changes in Benzene- Induced Acute Myeloid Leukaemia. Journal of Clinical Epigenetics, 2016, 2, .	0.3	4
49	Effects of multi-component mixtures of polyaromatic hydrocarbons and heavy metal/loid(s) on Nrf2-antioxidant response element (ARE) pathway in ARE reporter-HepG2 cells. Toxicology Research, 2016, 5, 1160-1171.	0.9	11
50	Effects of arsenic and cadmium on bioaccessibility of lead in spiked soils assessed by Unified BARGE Method. Chemosphere, 2016, 154, 343-349.	4.2	7
51	Continued Studies on the Effects of Simazine on the Liver Histological Structure and Metamorphosis in the Developing Xenopus laevis. Bulletin of Environmental Contamination and Toxicology, 2016, 97, 517-520.	1.3	5
52	Effects of binary mixtures of benzo[a]pyrene, arsenic, cadmium, and lead on oxidative stress and toxicity in HepG2 cells. Chemosphere, 2016, 165, 41-51.	4.2	33
53	Gene expression profiles in testis of developing male Xenopus laevis damaged by chronic exposure of atrazine. Chemosphere, 2016, 159, 145-152.	4.2	18
54	Bioaccessibility of arsenic and cadmium assessed for inÂvitro bioaccessibility in spiked soils and their interaction during the Unified BARGE Method (UBM) extraction. Chemosphere, 2016, 147, 444-450.	4.2	38

CHENG PENG

#	Article	IF	CITATIONS
55	The binary, ternary and quaternary mixture toxicity of benzo[a]pyrene, arsenic, cadmium and lead in HepG2 cells. Toxicology Research, 2016, 5, 703-713.	0.9	23
56	The Cotransplantation of Olfactory Ensheathing Cells with Bone Marrow Mesenchymal Stem Cells Exerts Antiapoptotic Effects in Adult Rats after Spinal Cord Injury. Stem Cells International, 2015, 2015, 1-13.	1.2	20
57	A review of non-exhaustive chemical and bioavailability methods for the assessment of polycyclic aromatic hydrocarbons in soil. Environmental Technology and Innovation, 2015, 4, 159-167.	3.0	16
58	Malathion-induced testicular toxicity is associated with spermatogenic apoptosis and alterations in testicular enzymes and hormone levels in male Wistar rats. Environmental Toxicology and Pharmacology, 2015, 39, 659-667.	2.0	76
59	Assessing Atrazine-Induced Toxicities in Bufo bufo gargarizans Cantor. Bulletin of Environmental Contamination and Toxicology, 2015, 94, 152-157.	1.3	9
60	BTEX in vitro exposure tool using human lung cells: Trips and gains. Chemosphere, 2015, 128, 321-326.	4.2	28
61	The Effects of Simazine, a Chlorotriazine Herbicide, on the Expression of Genes in Developing Male Xenopus laevis. Bulletin of Environmental Contamination and Toxicology, 2015, 95, 157-163.	1.3	21
62	Micronucleus formation by single and mixed heavy metals/loids and PAH compounds in HepG2 cells. Mutagenesis, 2015, 30, 593-602.	1.0	22
63	Toxic effects of individual and combined effects of BTEX on Euglena gracilis. Journal of Hazardous Materials, 2015, 284, 10-18.	6.5	54
64	Assessing benzene-induced toxicity on wild type Euglena gracilis Z and its mutant strain SMZ. Chemosphere, 2013, 93, 2381-2389.	4.2	11
65	Hanging drop: An in vitro air toxic exposure model using human lung cells in 2D and 3D structures. Journal of Hazardous Materials, 2013, 261, 701-710.	6.5	31
66	Genotoxicity of hydroquinone in A549 cells. Cell Biology and Toxicology, 2013, 29, 213-227.	2.4	32
67	CK2 phosphorylation-dependent interaction between aprataxin and MDC1 in the DNA damage response. Nucleic Acids Research, 2010, 38, 1489-1503.	6.5	53
68	Involvement of novel autophosphorylation sites in ATM activation. EMBO Journal, 2006, 25, 3504-3514.	3.5	251
69	Dramatic extension of tumor latency and correction of neurobehavioral phenotype in Atm-mutant mice with a nitroxide antioxidant. Free Radical Biology and Medicine, 2006, 41, 992-1000.	1.3	67
70	ATM and Cellular Response to DNA Damage. , 2005, 570, 457-476.		20
71	Functional consequences of sequence alterations in the ATM gene. DNA Repair, 2004, 3, 1197-1205.	1.3	55
72	Oxidative Stress Is Responsible for Deficient Survival and Dendritogenesis in Purkinje Neurons from Ataxia-Telangiectasia Mutated Mutant Mice. Journal of Neuroscience, 2003, 23, 11453-11460.	1.7	125

#	Article	IF	CITATIONS
73	Functional Link between BLM Defective in Bloom's Syndrome and the Ataxia-telangiectasia-mutated Protein, ATM. Journal of Biological Chemistry, 2002, 277, 30515-30523.	1.6	108
74	One-Step site-directed mutagenesis of ATM cDNA in large (20kb) plasmid constructs. Human Mutation, 2002, 20, 323-323.	1.1	27